

## System-size dependence of strangeness production in nucleus-nucleus collisions at $\sqrt{s_{NN}} = 17.3$ GeV

C. Alt,<sup>9</sup> T. Anticic,<sup>21</sup> B. Baatar,<sup>8</sup> D. Barna,<sup>4</sup> J. Bartke,<sup>6</sup> L. Betev,<sup>10,9</sup> H. Bialkowska,<sup>19</sup> A. Billmeier,<sup>9</sup> C. Blume,<sup>7,9</sup> B. Boimska,<sup>19</sup> M. Botje,<sup>1</sup> J. Bracinić,<sup>3</sup> R. Bramm,<sup>9</sup> R. Brun,<sup>10</sup> P. Bunčić,<sup>9,10</sup> V. Cerny,<sup>3</sup> P. Christakoglou,<sup>2</sup> O. Chvala,<sup>15</sup> J.G. Cramer,<sup>17</sup> P. Csató,<sup>4</sup> N. Dardenov,<sup>18</sup> A. Dimitrov,<sup>18</sup> P. Dinkelaker,<sup>9</sup> V. Eckardt,<sup>14</sup> G. Farantatos,<sup>2</sup> D. Flierl,<sup>9</sup> Z. Fodor,<sup>4</sup> P. Foka,<sup>7</sup> P. Freund,<sup>14</sup> V. Friese,<sup>7,13</sup> J. Gál,<sup>4</sup> M. Gaździcki,<sup>9</sup> G. Georgopoulos,<sup>2</sup> E. Gładysz,<sup>6</sup> K. Grebieszko,<sup>20</sup> S. Hegyi,<sup>4</sup> C. Höhne,<sup>13</sup> K. Kadija,<sup>21</sup> A. Karev,<sup>14</sup> M. Kliemant,<sup>9</sup> S. Kniege,<sup>9</sup> V.I. Kolesnikov,<sup>8</sup> T. Kollegger,<sup>9</sup> E. Kornas,<sup>6</sup> R. Korus,<sup>12</sup> M. Kowalski,<sup>6</sup> I. Kraus,<sup>7</sup> M. Kreps,<sup>3</sup> M. van Leeuwen,<sup>1</sup> P. Lévai,<sup>4</sup> L. Litov,<sup>18</sup> B. Lungwitz,<sup>9</sup> M. Makariev,<sup>18</sup> A.I. Malakhov,<sup>8</sup> C. Markert,<sup>7</sup> M. Mateev,<sup>18</sup> B.W. Mayes,<sup>11</sup> G.L. Melkumov,<sup>8</sup> C. Meurer,<sup>9</sup> A. Mischke,<sup>7</sup> M. Mitrovski,<sup>9</sup> J. Molnár,<sup>4</sup> St. Mrówczyński,<sup>12</sup> G. Pálla,<sup>4</sup> A.D. Panagiotou,<sup>2</sup> D. Panayotov,<sup>18</sup> A. Petridis,<sup>2</sup> M. Pikna,<sup>3</sup> L. Pinsky,<sup>11</sup> F. Pühlhofer,<sup>13</sup> J.G. Reid,<sup>17</sup> R. Renfordt,<sup>9</sup> A. Richard,<sup>9</sup> C. Roland,<sup>5</sup> G. Roland,<sup>5</sup> M. Rybczyński,<sup>12</sup> A. Rybicki,<sup>6,10</sup> A. Sandoval,<sup>7</sup> H. Sann,<sup>7,\*</sup> N. Schmitz,<sup>14</sup> P. Seyboth,<sup>14</sup> F. Siklér,<sup>4</sup> B. Sitar,<sup>3</sup> E. Skrzypczak,<sup>20</sup> G. Stefanek,<sup>12</sup> R. Stock,<sup>9</sup> H. Ströbele,<sup>9</sup> T. Susa,<sup>21</sup> I. Szentpétery,<sup>4</sup> J. Sziklai,<sup>4</sup> T.A. Trainor,<sup>17</sup> V. Trubnikov,<sup>20</sup> D. Varga,<sup>4</sup> M. Vassiliou,<sup>2</sup> G.I. Veres,<sup>4,5</sup> G. Vesztergombi,<sup>4</sup> D. Vranić,<sup>7</sup> A. Wetzler,<sup>9</sup> Z. Włodarczyk,<sup>12</sup> I.K. Yoo,<sup>16</sup> J. Zaraneck,<sup>9</sup> and J. Zimányi<sup>4</sup>

(NA49 Collaboration)

<sup>1</sup>NIKHEF, Amsterdam, Netherlands.

<sup>2</sup>Department of Physics, University of Athens, Athens, Greece.

<sup>3</sup>Comenius University, Bratislava, Slovakia.

<sup>4</sup>KFKI Research Institute for Particle and Nuclear Physics, Budapest, Hungary.

<sup>5</sup>MIT, Cambridge, MA, USA.

<sup>6</sup>Institute of Nuclear Physics, Cracow, Poland.

<sup>7</sup>Gesellschaft für Schwerionenforschung (GSI), Darmstadt, Germany.

<sup>8</sup>Joint Institute for Nuclear Research, Dubna, Russia.

<sup>9</sup>Fachbereich Physik der Universität, Frankfurt, Germany.

<sup>10</sup>CERN, Geneva, Switzerland.

<sup>11</sup>University of Houston, Houston, TX, USA.

<sup>12</sup>Świętokrzyska Academy, Kielce, Poland.

<sup>13</sup>Fachbereich Physik der Universität, Marburg, Germany.

<sup>14</sup>Max-Planck-Institut für Physik, Munich, Germany.

<sup>15</sup>Institute of Particle and Nuclear Physics, Charles University, Prague, Czech Republic.

<sup>16</sup>Department of Physics, Pusan National University, Pusan, Republic of Korea.

<sup>17</sup>Nuclear Physics Laboratory, University of Washington, Seattle, WA, USA.

<sup>18</sup>Atomic Physics Department, Sofia University St. Kliment Ohridski, Sofia, Bulgaria.

<sup>19</sup>Institute for Nuclear Studies, Warsaw, Poland.

<sup>20</sup>Institute for Experimental Physics, University of Warsaw, Warsaw, Poland.

<sup>21</sup>Rudjer Boskovic Institute, Zagreb, Croatia.

(Dated: August 13, 2005)

Emission of  $\pi^\pm$ ,  $K^\pm$ ,  $\phi$  and  $\Lambda$  was measured in near-central C+C and Si+Si collisions at 158 AGeV beam energy. Together with earlier data for p+p, S+S and Pb+Pb, the system-size dependence of relative strangeness production in nucleus-nucleus collisions is obtained. Its fast rise and the saturation observed at about 60 participating nucleons can be understood as onset of the formation of coherent systems of increasing size.

PACS numbers: 25.75.-q

Most recent experimental studies of particle production in relativistic nucleus-nucleus collisions have focussed on heavy reaction partners because of the expectation that the transition to a deconfined state of strongly interacting matter [1] is more likely to occur in large collision systems. However, earlier experiments with lighter beams at the CERN SPS accelerator had demonstrated that already in  $^{32}\text{S}+\text{S}$  collisions [2] relative strangeness production – which has been discussed as a possible indicator for such a transition [3] – is significantly enhanced

compared to p+p collisions and, as found later, is close to the situation in  $^{208}\text{Pb}+\text{Pb}$  [4, 5].

In order to understand the origin of this enhancement a systematic study of its dependence on the size of the collision system is required. In this Letter we discuss a systematic study of its dependence on the size of the collision system is required. In this Letter we discuss systems with similar geometry, i. e. near-central and approximately symmetric  $A+A$  collisions between nuclei of varying mass number  $A$ . New data on the production of  $\pi^\pm$ ,  $K^\pm$ ,  $\phi$ -mesons and  $\Lambda$ -baryons will be presented for the systems C+C and Si+Si. They were obtained with

the NA49 spectrometer at the CERN SPS at 158 AGeV beam energy, corresponding to a center-of-mass energy of  $\sqrt{s_{NN}} = 17.3$  GeV. The results will be discussed together with available data for p+p and Pb+Pb at 158 AGeV and S+S at 200 AGeV beam energy. It will be shown that strangeness enhancement develops fast with increasing size of the collision system reaching the level of Pb+Pb already at about 60 participating nucleons. We argue that this result can be understood assuming the formation of coherent systems of increasing size.

NA49 is a fixed-target experiment at CERN [6] using external SPS beams. For the present study a fragmented Pb beam of 158 AGeV was used [6]. The fragments were selected by magnetic rigidity ( $Z/A = 0.5$ ) and by specific energy loss in transmission detectors in the beam line. The "C-beam" as defined by the online and offline trigger was a mixture of ions with  $Z=6$  and 7 (intensity ratio 69:31) in the case of the meson measurements, and pure  $Z=6$  ions for the  $\Lambda$ . As "Si-beam" we used ions with  $Z=13,14$ , and 15 (35:41:24). 3 mm and 10 mm thick carbon targets (2.4% and 7.9% interaction length) were chosen, and a 5 mm thick Si target (4.4%). The veto calorimeter placed 20 m downstream of the target accepts nearly all beam particles, projectile fragments and spectator neutrons and protons [6]. By setting an upper threshold for the energy deposit, the  $(15.3 \pm 2.4)\%$  most central C+C and  $(12.2 \pm 1.8)\%$  most central Si+Si interactions were selected [7]. After all cuts typically 45k events were analyzed for the mesons and 200k for the  $\Lambda$ . Simulations based on the VENUS model of nucleus-nucleus interactions [8] allow to calculate impact parameter range and mean number of wounded nucleons [9]:  $b < 2.0$  fm for C+C and  $b < 2.6$  fm for Si+Si, for  $\langle N_{\text{wound}} \rangle$  see table II. In  $A + A$  reactions some nucleons in the collision may participate only through secondary cascading processes. In this paper, we do not include such nucleons in counting the number of wounded nucleons  $N_{\text{wound}}$ , but we do include them in the number of participating nucleons  $N_{\text{part}}$ , which is also provided by VENUS. These definitions differ from those assumed for Glauber calculations. For the  $N_{\text{part}}$  values given in table II the numbers from VENUS are averaged with those derived from the measured energy of the projectile spectators in the veto calorimeter.

Charged particles produced in beam-target interactions were measured in the NA49 large-acceptance hadron spectrometer consisting of magnets and time projection chambers (TPCs), two of them immediately behind the target and inside the magnetic field, two additional ones further downstream on both sides of the beam (for details see [6]). By tracking and measurement of the specific energy loss ( $dE/dx$ ) in the TPCs the momentum and the identity of the particles were determined. In the (lab)momentum range  $4 < p < 50$  GeV/c and with a relative  $dE/dx$  resolution ranging from about (3-6)% depending on track length and momentum [6] pi-

ons, kaons and protons could be resolved on a statistical basis by decomposing the  $dE/dx$  spectra in  $(p, p_t)$  bins which are then transformed to  $(y, p_t)$  or  $(y, m_t)$  bins ( $p_t =$  transverse momentum,  $m_t =$  transverse mass,  $y =$  c.m. rapidity). Within the geometrical acceptance of the spectrometer which covers most of the forward hemisphere in the center-of-mass system of the collision pions and kaons were selected in a range of the azimuthal angle (about 28% of  $2\pi$ ) where small background and a flat acceptance is ensured. Acceptance and corrections for in-flight decay of kaons (about 2% losses in addition) were determined by GEANT [10] simulations. The contribution of pions from weak decays of hadrons (mainly  $K_S^0$ ) is subtracted using events from the VENUS model (about 5%). Care is taken that the VENUS multiplicities agree with data, otherwise they are scaled accordingly. The  $\phi$ -mesons were measured via their strong decay into  $K^+K^-$  pairs (branching ratio 49.1%). Yields were derived in  $y$ - or  $p_t$ -bins from the corresponding peak in the  $K^+K^-$  invariant-mass spectra after subtracting the combinatorial background; the overall acceptance in the forward hemisphere amounts to about 45%. The technique is described in [11]; for more results also on the other mesons see [7].  $\Lambda$ -hyperons decay weakly via  $\Lambda \rightarrow p\pi^-$  (branching ratio 63.9%). They were identified on the basis of their typical V0 decay topology and the  $p\pi^-$  invariant mass; for the method see [5]. The  $p_t$ -integrated combination of acceptance and detection efficiency ranges from 8% in the most backward  $y$ -bin to about 57% at midrapidity. Since all  $\Sigma^0$  decay electromagnetically to  $\Lambda$ -baryons,  $\Lambda$  denotes the sum of both. For Si+Si an additional correction of  $(5 \pm 3)\%$  for the reduced  $\Lambda$  reconstruction efficiency was applied due to the higher track density in these reactions. GEANT simulations showed that, varying slightly with  $p_t$  and  $y$ , 90% of the  $\Lambda$ -baryons from weak decays of  $\Xi^-$  and  $\Xi^0$  contribute to the measured  $\Lambda$ -yield. Using yield estimates from statistical model fits [12] a feeddown correction of  $(9 \pm 3)\%$  and  $(10 \pm 3)\%$  was applied for  $\Lambda$  from C+C and Si+Si, respectively.

For all particles under study yields were obtained in  $(y, p_t)$  bins. The transverse distributions, those close to midrapidity being shown in fig. 1, were fitted with a thermal ansatz  $d^2N/(m_t dm_t dy) \propto \exp(-m_t/T)$ . The fit was used to extrapolate to  $p_t$ -regions not covered by the measurement, and the yield  $dN/dy$  was obtained by summing the measured bins and this extrapolation. The latter correction was of the order of a few percent typically. An exception were pions at midrapidity ( $-0.13 < y < 0.33$ ) for which the correction factors became as large as 2 to 3 due to the limit  $p < 4$  GeV/c for particle identification. In this case, spectral shapes from the NA35 S+S [13] measurements were used, this way taking the known low- $p_t$  pion enhancement into account. In order to estimate the systematic error in this phase space region different analysis strategies were investigated: When extrapolating the pion yields with a straight exponential

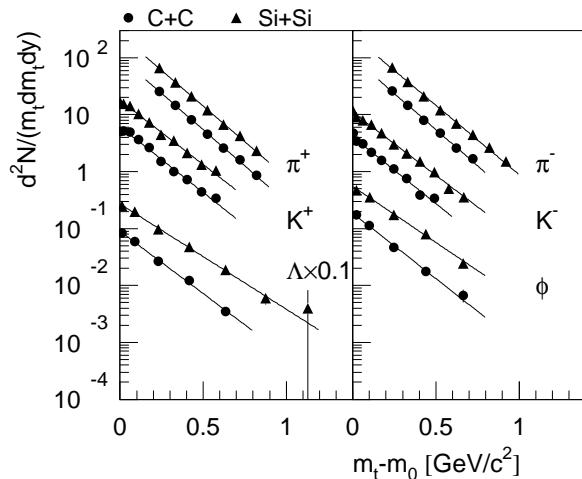


FIG. 1: Transverse mass distributions for  $\pi$  and  $K$  in  $0.1 < y < 0.33$ , for  $\phi$  averaged over  $0 < y < 1.8$ , and for  $\Lambda$  in  $|y| < 0.4$  measured in C+C ( $\bullet$ ) and Si+Si ( $\blacktriangle$ ) collisions. Only statistical errors are shown.

with an inverse slope  $T$  as given in table I, yields would be lower by (6-9)%. An  $h^-$  analysis as performed in [4] with corrections for  $K^-$  and  $\bar{p}$  gives (5-9)% higher yields. This uncertainty mainly determines the systematic error on the midrapidity and total pion yields. The pion rapidity distributions  $dN/dy$  (fig. 2) were approximated by a superposition of two Gaussians displaced symmetrically around mid-rapidity by a shift  $\pm y_0$ . For kaons and the  $\phi$ -meson a single Gaussian was used. Integration gives the total average yield  $\langle N \rangle$  of each particle. To obtain the yields of  $\Lambda$ -baryons their  $y$ -distribution was fitted by a shape adopted from p+p and S+S measurements. The mean of both approximations was taken for C+C; for Si+Si only the shape from S+S was used (lines in fig. 2). For the  $\phi$ -meson with its much lower abundance the  $p_t$ -distribution could only be obtained when averaged over a wider rapidity range,  $0 < y < 1.8$ . The values for  $dN/dy$  were determined in  $y$ -slices using the  $p_t$ -range  $0 < p_t < 1.5$  GeV/c and the averaged  $T$ -parameter for extrapolation (fig. 2).

Parameters for the kinetic distributions of all studied particles are given in table I, their yields in table II.

The strange-particle yields were normalized to the mean number of charged pions per event,  $\langle \pi^\pm \rangle = (\langle \pi^+ \rangle + \langle \pi^- \rangle)/2$ . In this way they represent the relative contribution of strange quarks in the final state. The results are shown in fig. 3 together with data for minimum-bias p+p [5, 11, 14] and Pb+Pb interactions (5% most central,  $\Lambda$ -baryons 10% most central) [4, 5, 11] taken at the same energy. The  $\Lambda$ -yield is scaled by the ratio of the number of wounded nucleons to account for the difference in the centrality selection, and the correction for feeddown from  $\Xi$ -baryons is applied [5]. Also plotted are the data for S+S (2% most central) obtained at the slightly higher energy of  $\sqrt{s_{NN}} = 19.4$  GeV [2].  $\Lambda$ -yields for S+S were

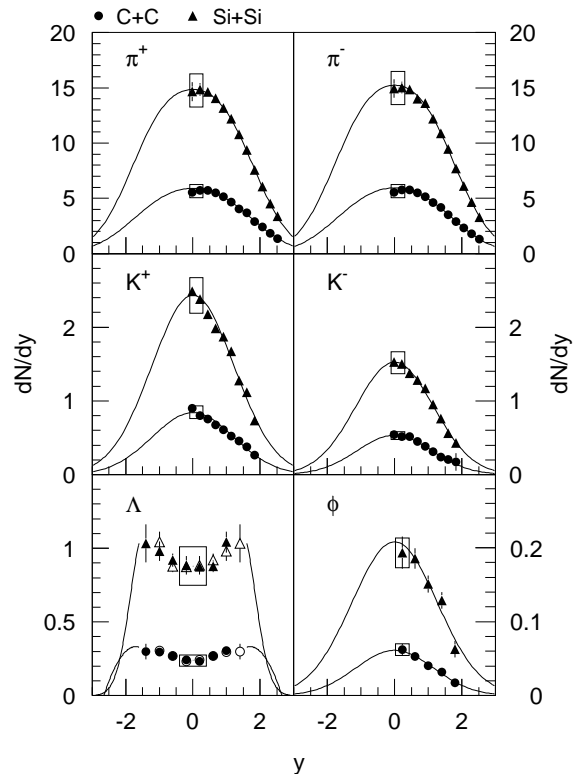


FIG. 2: Rapidity distributions for C+C ( $\bullet$ ) and Si+Si ( $\blacktriangle$ ) collisions. Open symbols are reflected at midrapidity. Error bars are statistical, systematic errors at midrapidity are indicated by the rectangular boxes. The curves represent fits to the data as described in the text.

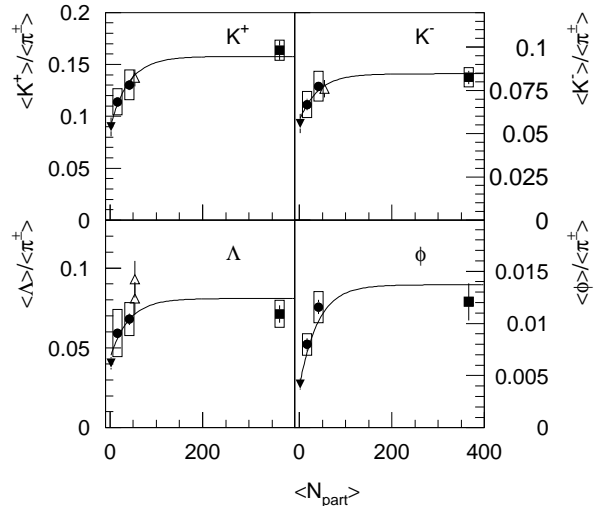


FIG. 3: Experimental ratios of  $\langle K^+ \rangle$ ,  $\langle K^- \rangle$ ,  $\langle \phi \rangle$ , and  $\langle \Lambda \rangle$  to  $\langle \pi^\pm \rangle$  plotted as a function of system size ( $\blacktriangledown$  p+p,  $\bullet$  C+C and Si+Si,  $\triangle$  S+S,  $\blacksquare$  Pb+Pb). Statistical errors are shown as error bars, systematic errors if available as rectangular boxes. The curves are shown to guide the eye and represent a functional form  $a - b \cdot \exp(-\langle N_{\text{part}} \rangle / 40)$ . At  $\langle N_{\text{part}} \rangle = 60$  they rise to about 80% of the difference of the ratios between  $N_{\text{part}} = 2$  and 400.

C+C	$T$ [MeV]	$dN/dy$	$\sigma_y$	$y_0$
$\pi^+$	$171 \pm 10$	$5.6 \pm 0.6$	$1.12 \pm 0.09$	$0.87 \pm 0.07$
$\pi^-$	$171 \pm 10$	$5.7 \pm 0.6$	$1.11 \pm 0.09$	$0.85 \pm 0.07$
$K^+$	$188 \pm 10$	$0.85 \pm 0.085$	$1.23 \pm 0.08$	
$K^-$	$185 \pm 10$	$0.53 \pm 0.053$	$1.10 \pm 0.09$	
$\phi$	$189 \pm 28$	$0.062 \pm 0.008$	$1.16 \pm 0.10$	
$\Lambda$	$199 \pm 15$	$0.24 \pm 0.038$		
Si+Si	$T$ [MeV]	$dN/dy$	$\sigma_y$	$y_0$
$\pi^+$	$173 \pm 10$	$14.8 \pm 1.5$	$1.04 \pm 0.08$	$0.91 \pm 0.07$
$\pi^-$	$178 \pm 10$	$15.0 \pm 1.5$	$1.05 \pm 0.08$	$0.89 \pm 0.07$
$K^+$	$192 \pm 10$	$2.4 \pm 0.24$	$1.24 \pm 0.08$	
$K^-$	$196 \pm 10$	$1.5 \pm 0.15$	$1.15 \pm 0.07$	
$\phi$	$220 \pm 28$	$0.19 \pm 0.02$	$1.27 \pm 0.10$	
$\Lambda$	$235 \pm 16$	$0.88 \pm 0.13$		

TABLE I: Parameters of the measured kinetic distributions. For pions and kaons  $T$  holds for  $0.1 < y < 0.33$ ,  $dN/dy$  for  $-0.13 < y < 0.33$ ; for  $\Lambda$  both values are given for  $|y| < 0.4$ . For the  $\phi$ -meson  $T$  is determined in  $0 < y < 1.8$ ,  $dN/dy$  in  $0 < y < 0.4$ . Only the dominating errors are given, i.e. statistical errors for the  $\phi$  and systematic errors for the other hadrons. Statistical errors of the latter are less than half the systematic error; for the  $\phi$  the systematic error is either the same ( $dN/dy$ ) or half of the statistical error.

	C+C	Si+Si
$\langle N_{\text{wound}} \rangle$	$14 \pm 2$	$37 \pm 3$
$\langle N_{\text{part}} \rangle$	$16.3 \pm 1$	$41.4 \pm 2$
$\langle \pi^+ \rangle$	$22.4 \pm 0.3 \pm 1.6$	$56.6 \pm 0.7 \pm 4$
$\langle \pi^- \rangle$	$22.2 \pm 0.3 \pm 1.6$	$57.6 \pm 0.6 \pm 4$
$\langle K^+ \rangle$	$2.54 \pm 0.03 \pm 0.25$	$7.44 \pm 0.08 \pm 0.74$
$\langle K^- \rangle$	$1.49 \pm 0.05 \pm 0.15$	$4.42 \pm 0.04 \pm 0.44$
$\langle \phi \rangle$	$0.18 \pm 0.01 \pm 0.02$	$0.66 \pm 0.03 \pm 0.08$
$\langle \Lambda \rangle$	$1.32 \pm 0.05 \pm 0.32$	$3.88 \pm 0.16 \pm 0.56$

TABLE II: Particle yields for C+C (15.3% most central collisions) and Si+Si (12.2%) at  $\sqrt{s_{NN}} = 17.3$  GeV. The first error is statistical, the second systematic.

scaled down by 10% to account for feeddown from  $\Xi$ -baryons assuming the same  $\Xi/\Lambda$  ratio as in Si+Si and using the information on the magnitude of the feeddown contribution given in [2].

Using the mean number of nucleons participating in the collision ( $\langle N_{\text{part}} \rangle$ ) as a measure of system size the resulting dependence of the relative strangeness production (fig. 3) is characterized by a fast rise at small  $\langle N_{\text{part}} \rangle$  values, reaching the level of Pb+Pb interactions at  $\langle N_{\text{part}} \rangle \sim 60$ . Note that the same shape of the enhancement curve holds for all measured strangeness-carrying particles including the  $\phi$ -meson with only hidden strangeness.

The system-size dependence of relative strangeness production indicates basic changes in the reaction mech-

anism due to the transition from an isolated N+N interaction to the situation in  $A + A$  where nucleons undergo several subsequent collisions within short time intervals and where many of these collision sequences occur close in space. Microscopic transport models such as UrQMD [15] calculate position and time of each collision in the center-of-mass system of the reaction. This allows to extract a collision density per unit space and time interval averaged over the interpenetration phase of the colliding nuclei. This collision density is found to increase with the size of the colliding nuclei; for central Si+Si reactions about 4-5 interactions per  $\text{fm}^3$  and  $\text{fm}/c$  are reached [7, 16]. It is reasonable to assume that neither the subsequent collisions nor the decay of the created objects proceed independently. We propose that the reaction volume should thus become quantum-mechanically coherent. Apparently, these conditions influence the global strangeness production rate.

Statistical models for hadron production (e.g. [17, 18]) are very successful in reproducing the particle ratios in p+p as well as in  $A + A$  collisions. In these models the implementation of strangeness conservation results in a strong volume dependence of strangeness production [19, 20, 21]. It is natural to invoke this effect, known as canonical strangeness suppression, as a qualitative explanation for the data shown in fig. 3. Quantitatively, however, discrepancies remain. In the model of Tounsi and Redlich [21], based on a hadronic scenario, as well as in the model of Rafelski and Danos [19], based on both, a partonic and a hadronic scenario, the strangeness saturation point (as defined in the caption of fig. 3) for  $|S| = 1$  particles is close to  $N_{\text{part}} = 10$ , in contrast to the experimental value of  $N_{\text{part}} = 60$ . One can reconcile theory with experiment assuming that only parts of the reaction volume form the statistical ensembles used in the models. This implies a modification of the linear relationship between volume and number of participants which was assumed so far.

To summarize, the data obtained for near-central symmetric nucleus-nucleus collisions with increasing number of participating nucleons show a steep rise of the relative strangeness content in the produced hadrons reaching a saturation value at around  $\langle N_{\text{part}} \rangle \sim 60$ . It is argued that this behavior is correlated with the formation of extended systems of dense and excited matter which collectively decay to the observed hadrons. Within the statistical model for hadron production this would qualitatively explain the increase of relative strangeness production, because the constraints due to strangeness conservation are diminishing with increasing size of the hadronizing systems. Strangeness saturation thus occurs when the grand-canonical limit can be applied [19, 20, 21, 22]. The experiment shows that for singly strange particles and the  $\phi$ -meson at  $\sqrt{s_{NN}} = 17.3$  GeV this happens already in central collisions between nuclei with  $A$  about 30.

This work was supported by the US Department

of Energy Grant DE-FG03-97ER41020/A000, the Bundesministerium für Bildung und Forschung, Germany, the Polish State Committee for Scientific Research (2 P03B 130 23, SPB/CERN/P-03/Dz 446/2002-2004, 2 P03B 04123), the Hungarian Scientific Research Foundation (T032648, T032293, T043514), the Hungarian National Science Foundation, OTKA, (F034707), the Polish-German Foundation, and the Korea Research Foundation Grant (KRF-2003-041-C00088).



\* deceased

- [1] J.C. Collins and M.J. Perry, Phys. Rev. Lett. **34**, 1352 (1975).
- [2] F. Karsch, Nucl. Phys. A **698**, 199c (2002).
- [3] J. Bartke et al., Z. Phys. C **48**, 191 (1990).
- [4] J. Bächler et al., Z. Phys. C **58**, 367 (1993).
- [5] T. Alber et al., Z. Phys. C **64**, 195 (1994).
- [6] J. Rafelski and B. Müller, Phys. Rev. Lett. **48**, 1066 (1982).
- [7] S.V. Afanasiev et al., Phys. Rev. C **66**, 054902 (2002).
- [8] T. Anticic et al., nucl-ex/0311024, Phys. Rev. Lett. **93**, 022302 (2004).
- [9] S. Afanasiev et al., Nucl. Instr. Meth. A **430**, 210 (1999).
- [10] C. Höhne, Ph.D. thesis, University of Marburg (2003), <http://archiv.ub.uni-marburg.de/diss/z2003/0627/>.
- [11] K. Werner, Phys. Rep. **232**, 87 (1993).
- [12] A. Białas, M. Błeszyński and W. Czyż, Nucl. Phys. B **111**, 461 (1976).
- [13] R. Brun et al., GEANT User Guide, 1986, CERN/DD/EE84-1.
- [14] S.V. Afanasiev et al., Phys. Lett. B **491**, 59 (2000).
- [15] F. Becattini, private communication.
- [16] T. Alber et al., Eur. Phys. J. C **2**, 643 (1998).
- [17] A.M. Rossi et al., Nucl. Phys. B **84**, 269 (1975).
- [18] S.A. Bass et al., Prog. Part. Nucl. Phys. **41**, 255 (1998). Version 1.2 was used in this work.
- [19] C. Höhne for the NA49 collaboration, Nucl. Phys. A **715**, 474c (2003).
- [20] P. Braun-Munzinger, J. Cleymans, H. Oeschler, K. Redlich, Nucl. Phys. A **697**, 902 (2002).
- [21] F. Becattini, M. Gazdzicki, A. Keränen, J. Manninen, R. Stock, Phys. Rev. C **69**, 024905 (2004).
- [22] J. Rafelski and M. Danos, Phys. Lett. B **97**, 279 (1980).
- [23] R. Hagedorn and K. Redlich, Z. Phys. C **27**, 541 (1985).
- [24] A. Tounsi and K. Redlich, J. Phys. G: Nucl. Part. Phys. **28**, 2095 (2002).
- [25] R. Stock, Phys. Lett. B **456**, 277 (1999).